

# MICROSCANNING XRF, XANES, AND XRD STUDIES OF THE DECORATED SURFACE OF ROMAN TERRA SIGILLATA CERAMICS

C. Mirguet,<sup>1</sup> P. Sciau,<sup>1</sup> P. Goudeau,<sup>2</sup> A. Mehta,<sup>3</sup> P. Pianetta,<sup>3</sup> Z. Liu,<sup>3</sup> and N. Tamura<sup>4</sup>

<sup>1</sup>CEMES-CNRS, 29 rue Jeanne Marvig BP 94347, 31055 Toulouse, France

<sup>2</sup>LMP-UMR 6630 CNRS, Université de Poitiers, SP2MI, Boulevard Marie et Pierre Curie, BP30179, 86962 Futuroscope Chasseneuil, France

<sup>3</sup>Stanford Synchrotron Radiation Laboratory, Stanford Linear Accelerator Center, Menlo Park, California 94025

<sup>4</sup>ALS-LBNL, 1 Cyclotron Road, Mail Stop 2-400, Berkeley, California 94720

## ABSTRACT

Different microscanning synchrotron techniques were used to better understand the elaboration process and origins of Terra Sigillata potteries from the Roman period. A mixture Gallic slip sample cross-section showing red and yellow colors was studied. The small (micron) size of the X-ray beam available at Stanford Synchrotron Radiation Laboratory (SSRL) and Advanced Light Source (ALS) synchrotron sources, coupled with the use of a sample scanning stage allowed us to spatially resolve the distribution of the constitutive mineral phases related to the chemical composition. Results show that red color is a result of iron-rich hematite crystals and the yellow part is a result of the presence of Ti-rich rutile-type phase (brookite). Volcanic-type clay is at the origin of these marble Terra Sigillata.

## INTRODUCTION

Terra Sigillata is the most famous fine ware of the Roman period. This ceramic is characterized by the redness of its body (or paste) and slip (or gloss), similar to the color of the clay (terra), and by the use of stamps (sigillata) in several cases. It was massively produced in standardized shapes and its widespread distribution made it one of the main groups of Roman potteries. Sigillata production can be seen as the industrial activity of specialized workshops. This class of pottery appeared in the middle first century BC in Italy at Arezzo. From the Augustan period (27 BC to 14 AD), it was widely spread within and outside the Italian Peninsula and branches were established in Pisa and in the south of Gaul. Then during the second century, new workshops appeared in the center of Gaul and in North Africa. The success of this pottery was mainly because of the brightness and color of the slip. Also in order to get a better insight into its technological “know-how,” microstructural and microchemical studies of the Gaul sigillata slip were performed by color measurements, transmission electron microscopy (TEM), and X-ray powder diffraction (XRD) measurements at ALS (Berkeley, California) [1–3]. The experimental methodology developed here—coupling synchrotron and TEM experiments—allows for the access of different scales presented in such complex and heterogeneous materials (see Figure 1). The microstructure of the slip is shown to be composed of a colorless glassy matrix integrating several crystalline phases: (1) inert grains of quartz that are residues of the raw clay used to make the slip, (2) Al-rich hematite crystals of micrometric scale developed during firing from the previously existing iron oxides, hydroxides, or both, and (3) newly developed Fe-rich corundum crystals of nanometric scale also developed during firing [3]. The glass matrix is mainly made of silicon and aluminium oxide without iron or other metallic ions so it is transparent and gives the characteristic shiny aspect of the slip. The red color is a result of iron which forms small hematite oxide crystals and which is also present in nanometric corundum crystals ( $\leq 7$  wt%). Iron presence in corundum should give a yellowish color to this phase,

as usually found in the gemological varieties of this mineral. But the main effect of corundum is to turn the slip into a very mechanically resistant coating. In summary, the color and specific properties of south Gaul Terra Sigillata are directly related to their microstructures.

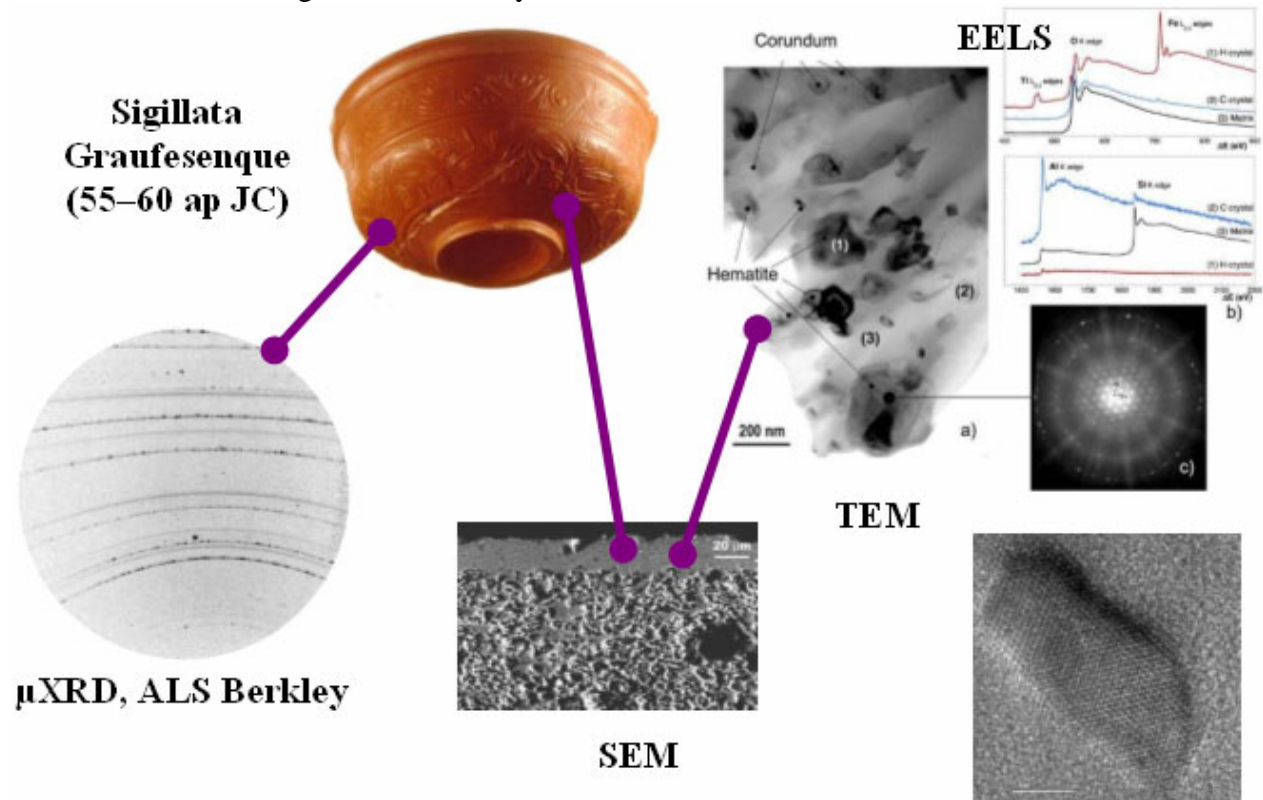


*Figure 1. To study these materials over a wide range of scales (nano, micro, and macro), a combination of different techniques is used: scanning electron microscopy (SEM), TEM (conventional, high resolution, and electron diffraction), electron energy loss spectroscopy (EELS), and XRD.*

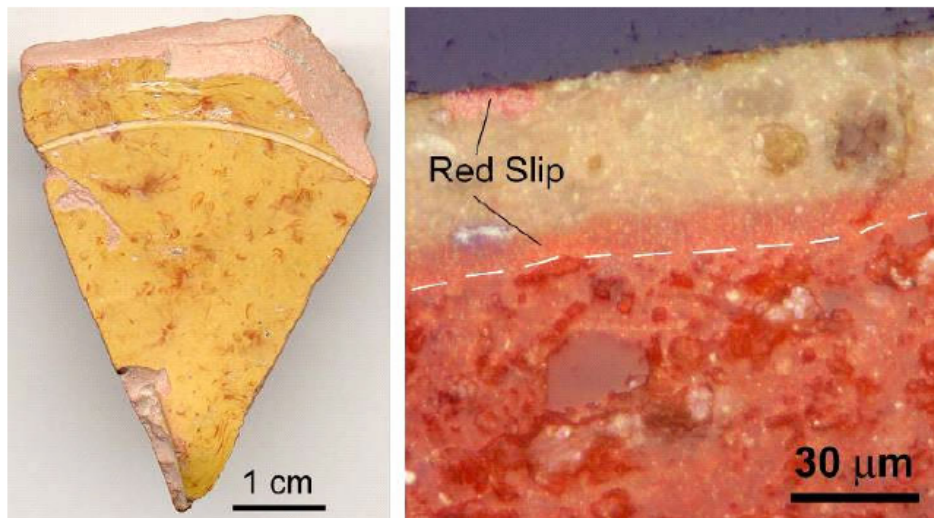


*Figure 2. Yellow/red mixture slip: (a) photography of a typical shred of marble sigillata and (b) corresponding cross section image obtained with an optical microscope. The dashed white line indicates the interface between the slip and the paste or body. The free surface is at the top.*

## **AIM OF THE STUDY**

During a short period, the largest Gallic workshop of La Graufesenque produced a very

particular type of sigillata with a yellow and red slip (see Figure 2). This type of production is not known in other Roman workshop. The red part was obtained from the clay used for the standard slip, but we have no information concerning the yellow component of mixture sigillata. In order to correlate the color aspect of the slip with mineralogical phases and element distribution in the slip, we decided to work on cross sectional samples [see Figure 2(b)] and then perform microscanning measurements at synchrotron facilities since the total thickness of the slip is about 30  $\mu\text{m}$  (less than 10  $\mu\text{m}$  for the red part) and thus beam sizes on the order of 1  $\mu\text{m}$  are necessary to get very precise correlation

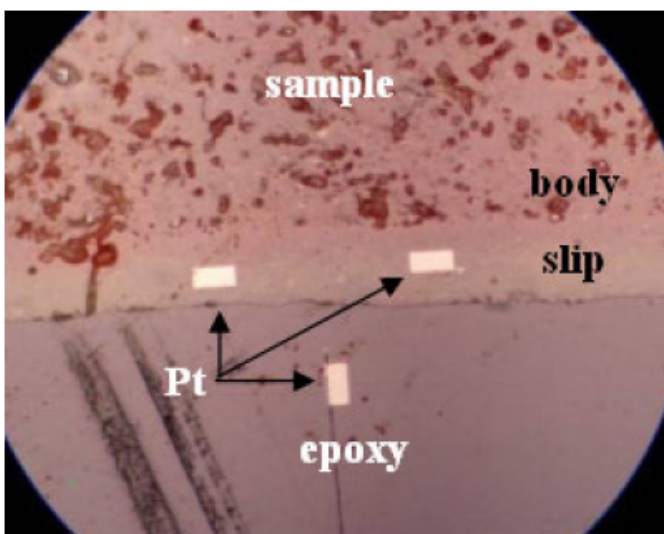


*Figure 3. Optical image showing the studied between element (Fe, Ti) and phase (hematite, sample cross section (top)—TSGMA, the epoxy corundum, or spinel) distributions. For easy resin (down), and the three Pt rectangular markers handling, the samples were embedded in an epoxy with dimension  $10 \times 30 \mu\text{m}^2$ .*

resin as shown in Figure 3 and also Figure 4(a) in the sample holder. Sample surfaces were cleaned prior to chemical analysis and cross sections were obtained by mechanical polishing.

## **MICROFOCUS EXPERIMENTS**

In order to achieve both chemical and structural analysis on the same sample, we applied for beam time at SSRL for fluorescence and absorption measurements in the frame work of a France – Stanford Center program and at ALS for micro-diffraction measurements since this is the only place in the world where switching from poly to monochromatic beam for micro-diffraction is available. An accurate comparison between structural maps measured by scanning micro-diffraction and chemical species maps obtained by fluorescence scans is difficult in our case because two different instruments are used for this purpose and located in two different synchrotron radiation facilities. This difficulty has been overcome by doing measurements on samples where areas delimited by three micrometric metallic markers (Pt rectangles) have been prepared by Focus Ion Beam (Figure 3).

Chemical (Fe, Ti, Ca) as well as Fe or Ti valence maps of the slip and the ceramic body are accessible thanks to micro-XRF and micro-XANES at SSRL beamline 2-3 using monochromatic beam and reflection mode. This experiment has been recently upgraded for doing principally fast fluorescence scans in case of low atomic element content and also, depending on the energy used, fast absorption scans. Effectively, the beamline flux at photon energies down to 5 keV (Ti K absorption edge) is very low and then the measured signal over background ratio is very low even if long recording times are achieved. Photography of the interior of the experimental hutch is given in Figure 4(b).

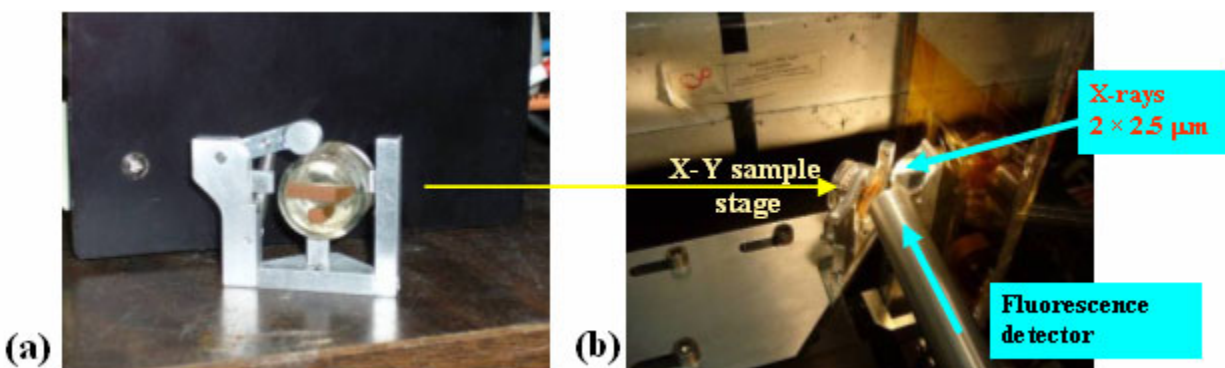


Figure 4. Microanalysis set up at SSRL beamline 2-3: (a) metallic sample holder containing the sample cross section embedded in epoxy resin and (b) inside of the SSRL BL2-3 experimental hut; the setup is composed of an X-Y sample stage, a fluorescence detector, and focusing optics.

The synchrotron XRD measurements were carried out on the new upgraded beamline 12.3.2 at ALS using either white beam or monochromatic beam in reflection mode (see Figure 5). The small (micron) size of the X-ray beam coupled with the use of a sample scanning stage allows one to spatially resolve the distribution and other characteristics of the constitutive mineral phases [4–6]. Kirkpatrick-Baez mirrors system provides us with submicron X-ray spot size. The remaining end station components are the four-crystal monochromator, fluorescence, and X-ray CCD detectors. The sample is placed on an X-Y sample stage. Notice that fluorescence detector is useful for finding markers at the sample surface and thus for calibrating the X-Y stage. All motors are computer control and dedicated software namely XMAS allows scanning measurements as well as data treatment for extracting phase information.

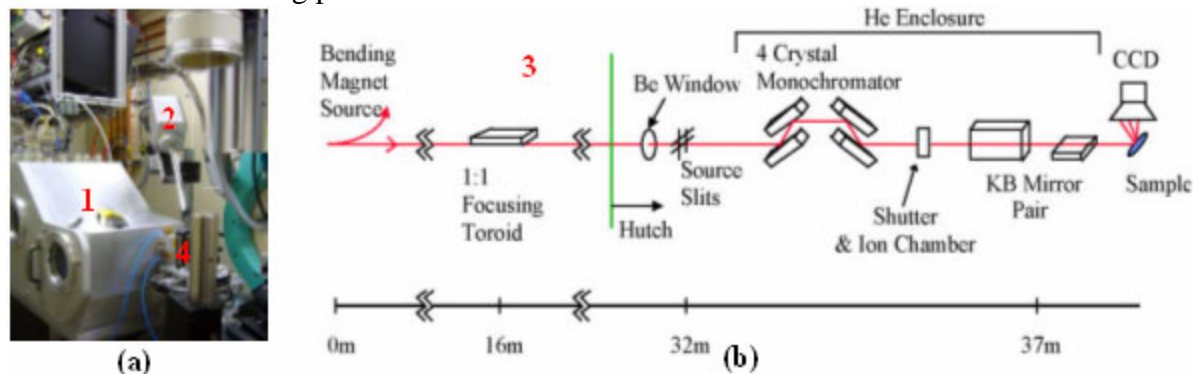


Figure 5. Micro-diffraction beam line at ALS (see <http://xraysweb.lbl.gov/microdif>): (a) photograph of the experimental hut showing the tank (1) under primary vacuum containing all the optics, the fluorescence detector (2), the CCD camera (3) for recording diffraction pattern, and the sample holder (4); (b) schematic drawing of the beamline 7.3.3 before upgrading (move from the bending magnet end-station 7.3.3 to the superbend beamline 12.3.2).

Collecting micro-EXAFS and micro-diffraction patterns for selected locations based on the chemical and valence map, we are able to determine the phase chemistry and local coordination of environment of Fe associated with grain size and phase structure. The microanalysis measurements at SSRL were successfully done on the first days of July 2007, but the micro-diffraction experiments scheduled at end of June 2007 at ALS were cancelled since the commissioning of the upgraded beamline was not yet achieved; our experiments were then postponed to the end of November 2007. Now, the measurements have been done successfully at the new ALS beamline and we are presenting the first results of a complete study using both techniques.



## RESULTS AND DISCUSSION

The X-ray beam size was  $2 \times 2.5 \mu\text{m}^2$  at the sample surface concerning microanalysis measurements. Several cross sectioned samples were measured using fast fluorescence scans (20 min) for several elements contained in the slip and the body (Fe, Ti, K, Ca). Additional oxidation state maps for iron ( $\text{Fe}^{3+}$  and  $\text{Fe}^{2+}$ ) were done using three energies close to the iron K absorption edge with reasonable recording time (between 6 and 10 h, depending on the step used and the dimension of the scan). XANES measurements have also been done at different points in the slip and the body. Concerning the Ti K edge, several tests have been done in Ti enriched region of the sample, but the flux at the beamline is not actually optimized for that low energy (close to 5 keV) and thus the XANES signal is still very noisy with a very long recording time.

Very interesting valence maps for iron were obtained during the shifts as illustrated in Figure 6 in the case of a comparison study of Gallic and Italic sigillata. This example was chosen because the obtained results demonstrate clearly the powerfulness of such measurements.

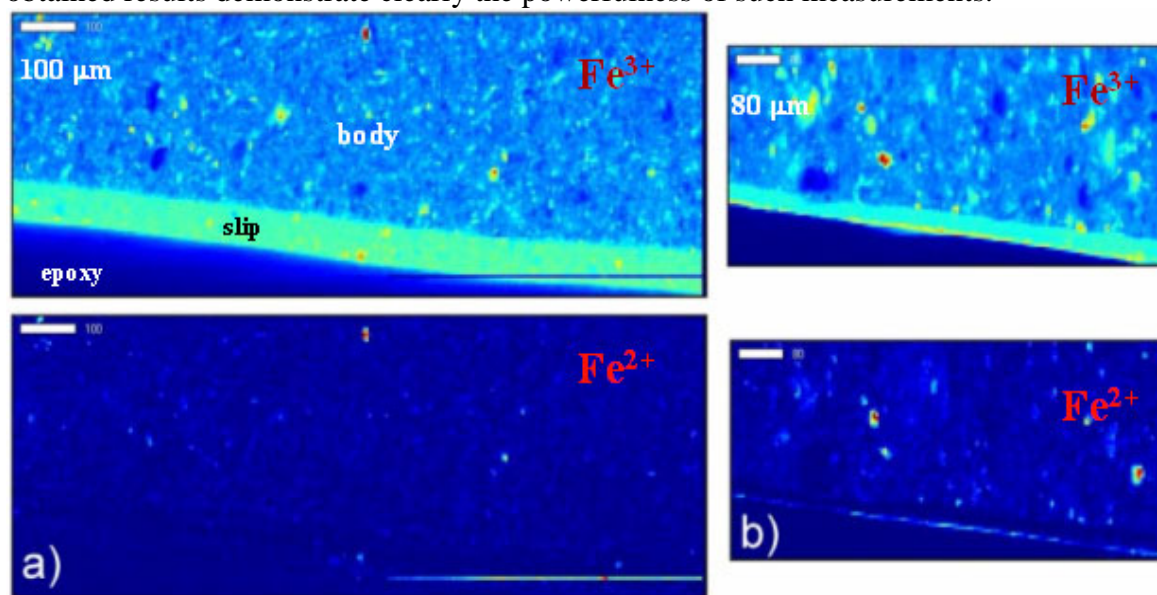


Figure 6. Comparison between  $\text{Fe}^{3+}/\text{Fe}^{2+}$  valence maps measured on (a) Gallic and (b) Italian ceramic cross sections.

Several interesting observations can be made when we comparing the two sets of maps. First, the iron distribution in the Italian slip is highly homogeneous compared to the Gallic one: the Italian potters used very fine clay particles in solution to prepare the slip at the pottery surface by “dip coating.” Therefore, the slip thickness is thinner for Italian potteries. The second information is related to the paste. The iron distribution is more heterogeneous for the Italian compared to the Gallic. Finally,  $\text{Fe}^{2+}$  is not evidenced in the Gallic slip but it is found at the surface of Italic slip. These findings seem to indicate that furnaces built by the Gallic potters were better performing. However, surface alteration because of aging and environmental aggressions or other artifacts related to production may also lead to the same results. Therefore more similar measurements on several samples are needed to confirm these preliminary results.

Concerning marble sigillata, chemical maps are represented in Figure 7(a); the platinum markers are clearly visible on the top map and other maps reveal the heterogeneous character of the body (paste), but also the slip when looking more precisely to the iron distribution map. A few local zones are Ti rich, and we performed the mineralogical maps [Figure 7(b)] with X-ray diffraction in such regions.

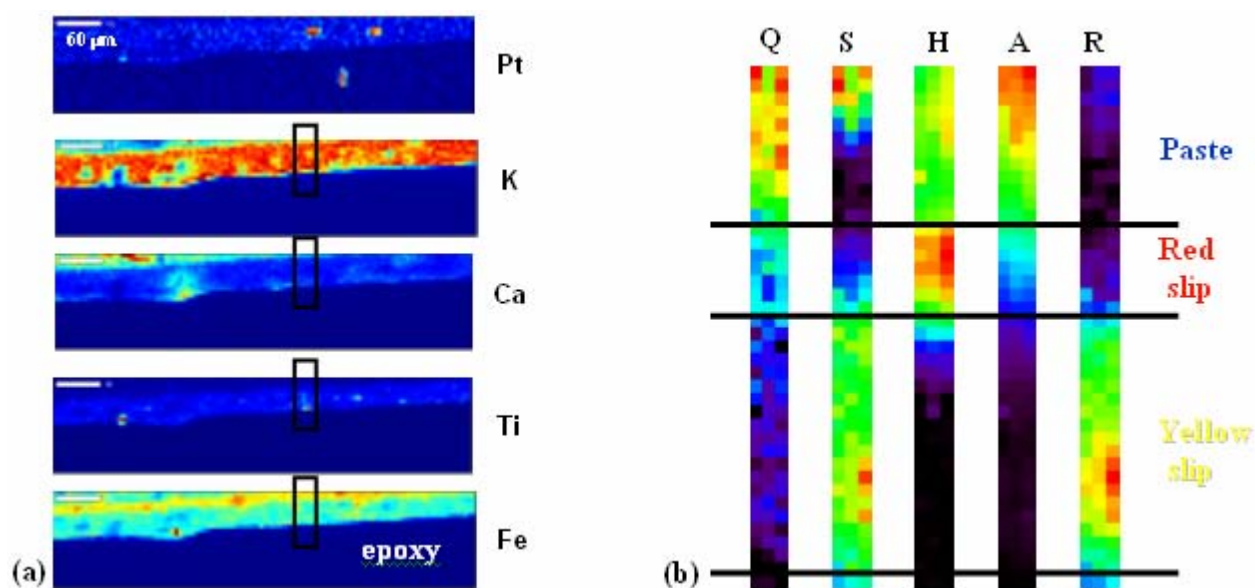


Figure 7. Micro X-ray beam mapping for (a) chemical and (b) phase investigations in marble Terra Sigillata cross section. The different analyzed chemical species are indicated in (a) as well as the mineralogical phases (Q: quartz; S: spinel; H: hematite; A: anorthite; R: rutile or titanium oxide) and the interfaces position in the cross section in (b). Right maps correspond to the black rectangle drawn on the left maps.

The phase maps are obtained after analyzing diffraction pattern recorded with monochromatic beam energy of 8.75 keV and an incident angle of 15° (interface perpendicular to the horizontal X axis), thanks to XMAS software. The recording time for a complete map was between 6 and 12 h. We clearly see that the red part is directly correlated with hematite but the yellow zone is constituted of spinel and rutile-type phases in agreement with chemical maps. Quartz and anorthite phases are present only in the paste. These results combined with others obtained very recently (April 2008) through TEM analysis show that the phase giving rise to the yellow color is in fact a pseudo-brookite structure which is close to the rutile structure (orthorhombic type)  $\text{Fe}_2\text{TiO}_5$  (50%  $\text{Fe}_2\text{O}_3$  + 50%  $\text{TiO}_2$ ). The clays used by the ancient potters were certainly Ti-rich volcanic-type, but the firing protocol used remained the same (vitrified slip up to 1000 °C). This production was very particular (middle of first century during a short period and only at La Graufesenque workshop); ancient potters certainly wanted to fabricate another type of pottery keeping the shapes and elaboration process of true sigillata but its marketing was certainly not successful. Some examples of such potteries are visible in a few museums in cities like Lisbon and Berlin. All these assumptions need to be verified by measuring other marble sigillata pot sherds found in the same workshop.

## CONCLUSION

The first results obtained during these experiments are promising. However, the penetration depth of X-rays may be a problem when working on thick sample cross sections (averaged in depth information) and we are now engaged to study thin cross section foils obtained thanks to Focused Ion Beam apparatus available at CEMES, Toulouse, France. These very thin samples are also studied by TEM.

## ACKNOWLEDGMENTS

The authors thank G. Benassayag and S. Webb for sample preparation using FIB technique at CEMES and for assistance during experiments at SSRL beamline 2-3, respectively. This work has been partly supported by a France–Stanford Center grant for the 2006–2007 academic years and the Director, Office of Science, Office of Basic Energy Sciences, of the U.S. Department of Energy who

is operating ALS and SSRL under Contract No. DE-AC02-05CH11231 and Contract No. DE-AC02-76-SFO0515, respectively.

## **REFERENCES**

- [1] Sciau, Ph.; Relaix, S.; Roucau, C.; Kihn, Y.; Chabanne, D. J. Am. Ceram. Soc. 2006, 89, 1053–1058.
- [2] Sciau, Ph.; Goudeau, Ph.; Tamura, N.; Dooryhee E. Appl. Phys. A: Mater. Sci. Process. 2006, 83, 219–224.
- [3] Sciau, Ph.; Relaix, S.; Mirguet, C.; Goudeau, Ph.; Bell, A. M. T.; Jones, R. L.; Pantos, E. Appl. Phys. A: Mater. Sci. Process. 2008, 90, 61–66.
- [4] Lynch, P. A.; Tamura, N.; Lau, D.; Madsen, I.; Liang, D.; Strohschnieder, M.; Stevenson, A. W. J. Appl. Crystallogr. 2007, 40, 1089–1096.
- [5] Harbottle, G.; Gordon, B. M.; Jones, K. W. Nucl. Instrum. Methods Phys. Res., Sect. B 1986, 14, 116–122.
- [6] Dooryhée, E.; Anne, M.; Bardiès, I.; Hodeau, J.-L.; Martinetto, P.; Rondot, S.; Salomon, J.; Vaughan, G. B. M.; Walter, P. Appl. Phys. A: Mater. Sci. Process. 2005, 81, 663–667.